Springer

KSME

Journal of Mechanical Science and Technology 24 (4) (2010) 999~1005
www.springerlink.com/content/1738-494x
DOI 10.1007/s12206-010-0213-y

Response of passive scalar to momentum disturbance in a transpired channel with wall injection †

Dongshin Shin[1] and Yang Na[2,*]

[1]*Department of Mechanical Engineering, Hongik University, Seoul, 121-791, Korea*
[2]*Department of Mechanical Engineering, Konkuk University, Seoul 143-701, Korea*

(Manuscript Received December 28, 2009; Revised February 10, 2010; Accepted February 12, 2010)

Abstract

In a transpired channel, the response of turbulent field to the external concentrated momentum forcing was investigated. The flow was characterized by a strong shear layer resulting from the interaction of the main flow with the injected mass at the surface. The time scale of the shedding vortex was imposed on the external disturbance to study the subsequent evolution of the resulting flow near the surface. The imposed time characteristics were persistent in the pressure field, but the amplification of instability was not evident in the present configuration. In contrast with pressure, the effect of external disturbance was not clearly exhibited in the temperature field near the surface. This is considered to be due to the dissimilarity between the turbulent velocity and the temperature fields in the presence of wall injection. Thus, it is expected that the perturbed near-wall heat transfer characteristics should be modeled in a different way from that of the velocity field.

Keywords: Concentrated disturbance; Large eddy simulation; Passive scalar; Transpired channel; Wall injection

1. Introduction

Hybrid rocket is receiving much attention these days due to its several advantages over the conventional rocket system, the first among which is the superiority of its safety features. In addition to this apparent merit, the potential of the sounding rocket and low-cost tactical missiles can be attributed to their low development cost and low temperature sensitivity advantages over their traditional solid and bipropellant counterparts. Nonetheless, despite the overwhelming experimental studies on hybrid rockets since the 1990s, their relatively lower density specific impulse compared with that of the solid rocket motor must be further improved to be widely used in a practical propulsion system.

Most of the pioneering investigations relevant to hybrid system dealt with non-turbulent weak injection [1-3]. However, although they demonstrated that pressure force can be greater than the turbulent shear stress, the velocity profile they obtained did not deviate much from that derived theoretically by Culick [4]. Since then, much effort has been made on fully turbulent cases, but most of the works are more inclined towards enhancing the regression rate by using various different fuel combinations and metal particle additives [5] than by obtaining velocity information. The insufficiency of turbulent flow field data is possibly due to the lack of proper instrumentation in such a very complex system.

Alongside the proliferation of advanced computer resources, numerical studies have likewise been conducted. Most of the earlier numerical works [6-8] employed the Reynolds stress or k-ε models to solve the turbulent flow. Their success was somewhat limited due to the restricted capability of the Reynolds Averaged Navier-Stoke (RANS) approach. More recently, several numerical investigations based on large eddy simulation (LES) on non-reacting flows have been performed in numerical geometry relevant to the solid motor. Although serious idealizations had to be introduced due to the prohibitively large computational cost, more detailed flow field information on turbulent field has been reported. One of the key issues in the context of turbulent flow field is the hydrodynamic stability because the steady operation of a rocket, which is one of its very important missions, is closely related to various flow instabilities. Apte and Yang [9, 10] documented very useful information on turbulence development and acoustic excitation process in a solid motor with one end closed. On the contrary, although their studies can be considered one of the most realistic numerical works to date, flow physics is not likely to be the same as in a hybrid motor due to the absence of the convection effect of an oxidizer stream. More recent

† This paper was recommended for publication in revised form by Associate Editor Haecheon Choi

*Corresponding author. Tel.: +82 2 450 3467, Fax.: +82 2 447 5886
E-mail address: yangna@konkuk.ac.kr

works by Na and Lee [11], Lee and Na [12], and Na [13] showed very interesting features of flow modification near the fuel surface in a transpired channel. Due to the interaction of the main oxidizer flow with the wall injected flow, turbulent structures are significantly altered, and isolated cell-like contours of streamwise velocity reminiscent of dark spots observed in the combustion tests [5] are produced near the surface. Likewise, it was shown that vortex shedding with a specific frequency was produced due to hydrodynamic instability.

Several earlier LES results for solid rocket showed that the onset of hydrodynamic instability could significantly change the unsteady flow evolution, but only few works were performed on a hybrid motor. Thus, it would be quite interesting to know what would happen if external perturbations are coupled with hydrodynamic instability in a hybrid rocket. Motivated by this issue on flow instability, a LES study was conducted to determine how the hydrodynamic instability affects the velocity and temperature fields in the hybrid combustion. Focus was given on the near-wall modification of turbulent field considering the external disturbances with a specified frequency using the LES technique. Disturbance was generated in terms of momentum forcing, and subsequent evolution of turbulent field including passive scalar was analyzed. To better focus on the near-wall turbulent flow with an acceptable computational cost, a hybrid motor was idealized with a transpired channel where the regression process was represented by a mass injection at the surface without combustion. Temperature was regarded as a passive scalar, with the Prandtl number being 1.

2. Numerical methodology

2.1 Governing equation

A typical hybrid motor is operated with a Mach number less than 0.1, and thus the effect of density variation can be neglected. With the assumption of cold flow, the combustion is not considered, and all the fluid parameters remain constant. Furthermore, the temperature is regarded as a passive scalar to solve the following set of filtered non-dimensional governing equations for velocity and temperature on a rectangular staggered grid:

$$\frac{\partial \overline{u_i}}{\partial x_i} = 0 \tag{1}$$

$$\frac{\partial \overline{u_i}}{\partial t} + \frac{\partial}{\partial x_j}(\overline{u_i}\,\overline{u_j}) = -\frac{\partial \overline{p}}{\partial x_i} + \frac{\partial}{\partial x_j}(2\nu \overline{S_{ij}} - \tau_{ij}) \tag{2}$$

$$\frac{\partial \overline{T}}{\partial t} + \frac{\partial}{\partial x_j}(\overline{u_j}\,\overline{T}) = \frac{\partial}{\partial x_j}(\alpha \frac{\partial \overline{T}}{\partial x_j} - q_j) \tag{3}$$

To close the system, residual stress tensor $\tau_{ij} = \overline{u_i u_j} - \overline{u}_i \overline{u}_j$ and residual heat flux vector $q_j = \overline{Tu_j} - \overline{T}\,\overline{u}_j$ were modeled using a dynamic mixed model (DMM). The details of solving the above set of governing equations were explained by Na and Lee [12] and Na [14].

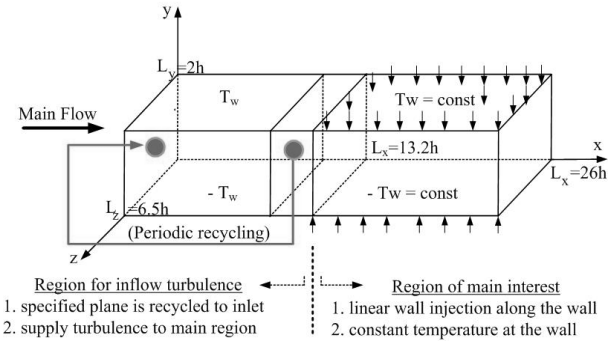

Fig. 1. Schematic of the computational domain.

2.2 Computational geometry

A hybrid motor was idealized with a transpired channel where the regression process was represented by the mass injection along the surface. Thus, the numerical domain consists of two different regions, as shown in Fig. 1. The streamwise extent of the domain is L_x=26h and the spanwise extent is L_z=6.5h, where h is the half-channel height.

The region dedicated for generating inflow turbulence was placed in front of the region of main interest where the wall injection was applied. To provide realistic turbulence to the main region, the flow field information given in the specific plane was recycled to the inlet [15]. Note that the distance between these two planes were much larger than the length scale of the large eddies in the flow direction.

The geometry of the present flow contains several regions of non-negligible gradients in the wall-normal direction due to the mixing of the main oxidizer flow with the wall injection. The occurrence of a strong shear layer away from the wall is a direct consequence of the Kelvin-Helmholtz-type instability, which imposes a distinct time scale. Thus, a grid independence study was conducted, and the 1025x193x513 grid system believed to be reasonably good enough for the present work was selected [12].

To make the present analysis realistic, Reynolds number based on the inlet bulk velocity of the oxidizer and the half channel height was set to 22,500, which is very close to that of the accompanying experiment [12]. In the main region, the linearly increasing wall blowing was prescribed following the observation of several experiments [5, 12]. Thus, the wall normal velocity changed from the 1% of the inlet bulk velocity at x/h=13 to 3% at exit. A periodic boundary condition was applied in the spanwise direction and convective boundary condition was used at exit. For the energy equation, temperature was assumed to be constant on both upper and lower walls. Details of the numerical calculations and the grid system can be found in reference [12].

2.3 Concentrated momentum forcing

The fact that the flow inside the rocket motor is extremely sensitive to external disturbance is due to its intrinsic instability. In the present geometry similar to a typical dump combus-

tor, Kelvin-Helmholtz-type instability develops, and a subsequent vortex shedding characterizes the flow. Given the basic flow instability, checking the response of the turbulent flow near the wall surface to the external disturbance is very important. While various kinds of white noise provided to the propulsion system can be modeled as distributed forcing, external excitation resulting from the geometry of the injector can be treated as concentrated forcing characterized by a narrow band frequency. Possibly, there are many different ways of imposing external forcing, but the method of imposing a momentum disturbance is chosen here because of its convenience in the context of the present numerical algorithm. To minimize the destruction of the physically realistic turbulence supplied to the computational domain of main interest, the manipulation of the flow was done in the recycled channel.

Among the several possible methodologies, an attempt at prescribing an external momentum forcing of a specified frequency ($\omega h/U_b$ =8.5 in the current study) at the inlet was made. The reason for the choice of specific frequency of $\omega h/U_b$=8.5 is because the present flow configuration exhibited the given time characteristics [11-13]. Thus, the objective of the present work is to analyze the response of the flow to this external concentrated forcing to determine if this small disturbance can lead to the sudden amplification of instability, such as the DC-shift phenomenon.

Instead of introducing a momentum forcing term in the governing equation, streamwise velocity was disturbed by adding a velocity increment in the form of $\sum_n c_n a_n(y)\cos_n(\omega_n t)$, as indicated in Eq. (4). Thus, the pressure and the rest of the velocity components were adjusted to satisfy the governing equations.

$$u(y,z,t)|_{x=0} = u(y,z,t)|_{recycled\cdot plane} + \sum_n c_n a_n(y)\cos(\omega_n t) \quad (4)$$

To minimize the effect of the artificial manipulation of the flow, Eq. (4) was executed only at the inlet of the domain, and the magnitude of the disturbance was forced to remain low compared with the base flow. It is believed that the flow evolves sufficiently in the recycling region, enabling it to recover from this numerical manipulation. An adjustable constant c_n defines the strength of the intended forcing and was set to 0.01. Another constant $a_n(y)$ was introduced to consider geometrical variations of the rms of streamwise velocity, $u_{rms}(y)$.

3. Effect of concentrated forcing

Instantaneous and averaged flow fields will be presented here. For statistical results, variables were averaged over time and in a homogeneous spanwise direction, such that results were a function of both *x* and *y*.

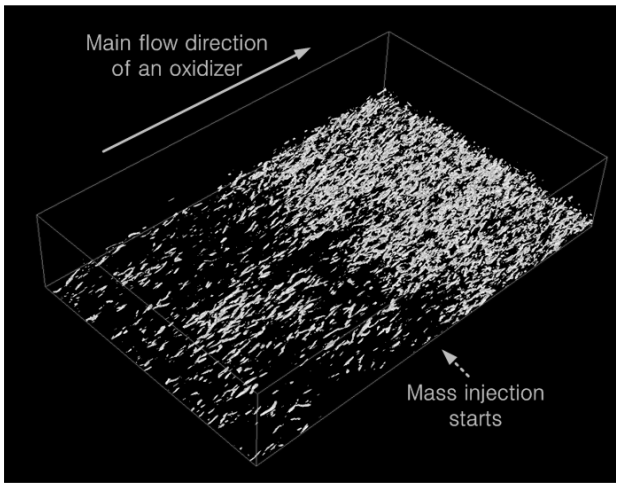

(a)

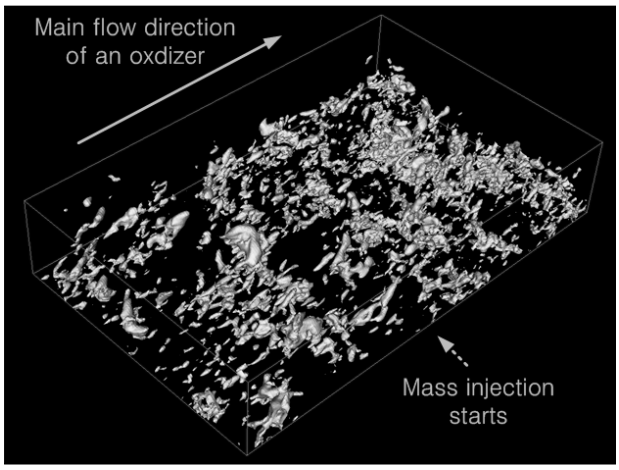

(b)

Fig. 2. Turbulent structures when external disturbance is imposed: (a) Iso-contours of turbulent structures; (b) Iso-contours of negative pressure fluctuation (p'= -1.13×10^{-2}).

3.1 Modification of turbulent structures

The turbulent structures and pressure fluctuations after imposing the concentrated momentum forcing are shown in Fig. 2. Turbulent structures were detected using the vortex identification method [16]. It should be noted that the density of turbulent structures increased abruptly after the wall blowing started. This is because the shear layer resulting from the interaction of the main flow with the injected mass at the surface was formed away from the wall. Kinematic configuration of turbulent structures was altered, such that the head of the structures is lifted away from the wall due to the action of wall injection. Iso-contours of pressure fluctuations are also displayed at the same location in Fig. 2(b). The negative value of pressure fluctuation was selected to conjecture the vertical structures. In this figure, a rapid variation of structures is not obvious, but an occurrence of a pseudo-periodic temporal

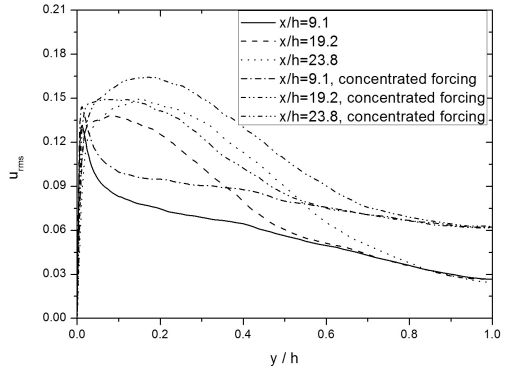

(a)

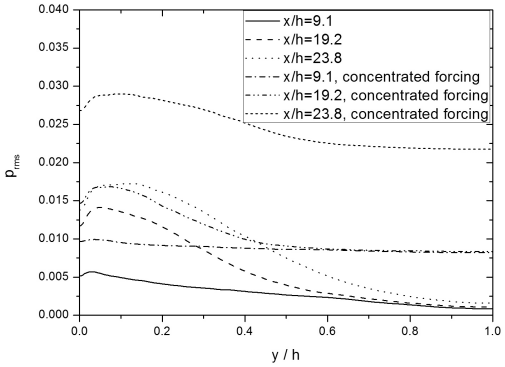

(b)

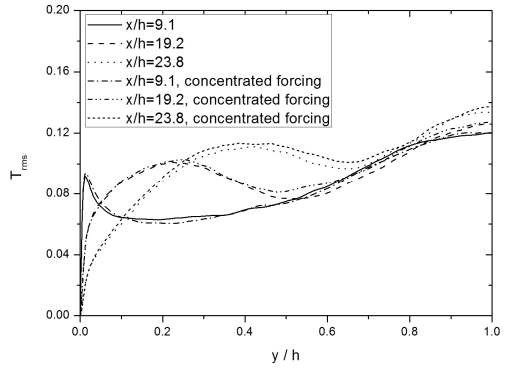

(c)

Fig. 3. Turbulence intensity: (a) streamwise velocity fluctuations; (b) pressure fluctuations; (c) temperature fluctuations.

behavior can be seen in the latter.

Fig. 3(a) shows how turbulence intensity increases due to the added disturbance. Throughout the channel height, external disturbance results in the significant increase in turbulence energy. More drastic changes were found in pressure intensity, as shown in Fig. 3(b). In all represented locations, intensities increased by factor 2. With the present level of excitation, disturbance did not lead to disastrous instability, such as resonance, but left the possibility of sudden amplification. A somewhat interesting result was obtained from the temperature field. In contrast with velocity and pressure, temperature intensity did not increase significantly, as illustrated in Fig. 3(c). Even in the region far away from the wall where the effect of injection is less felt, the level of intensity hardly changed. This suggests that the effect of non-negligible damping mechanism exists in the temperature field, allowing the external disturbance introduced in the velocity field to decay very rapidly. Considering the fact that a higher heat flux is required for a higher regression rate, a simple excitation may not be efficient for enhancing the convective heat transfer rate.

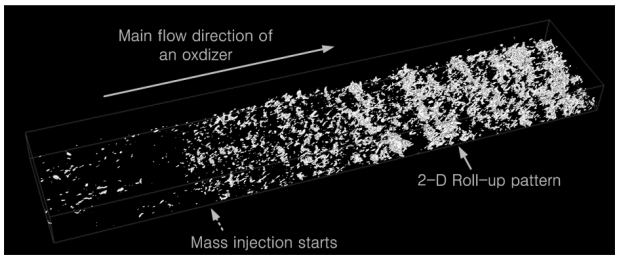

(a)

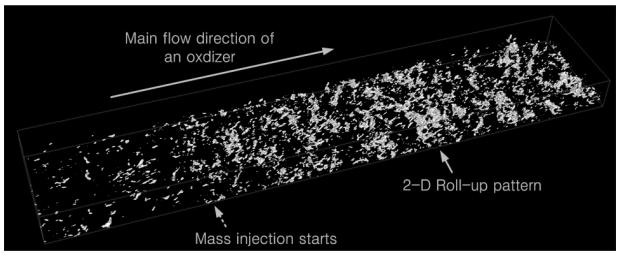

(b)

Fig. 4. Iso-contours of negative pressure fluctuation; (a) case without forcing; (b) case with forcing.

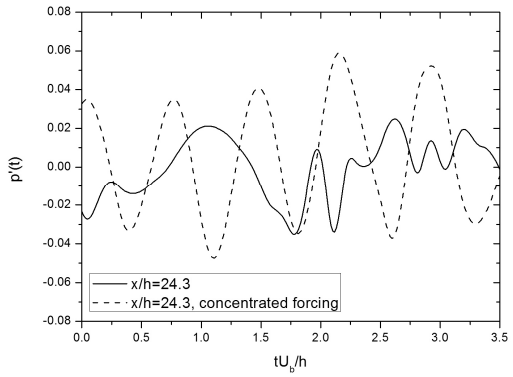

Fig. 5. Time history of pressure fluctuation with and without forcing.

The roll-up process due to the detached shear layer can be displayed by the contours of negative pressure fluctuation. Two-dimensional roller-like structures are evident for the case without forcing in Fig. 4(a). As the flow moves downstream, Kelvin Helmholtz-type instability causes a periodic shedding of vortical structures as detected by the low pressure region. In the presence of external disturbance, the coherence of vortical structure appears to decrease in Fig. 4(b), but the occurrence

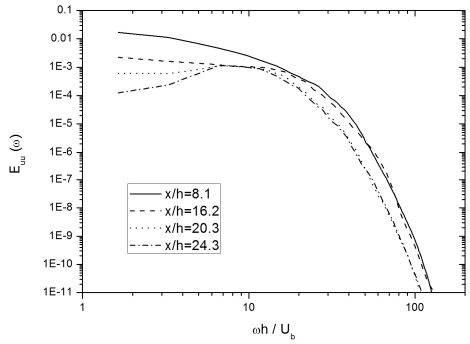

(a)

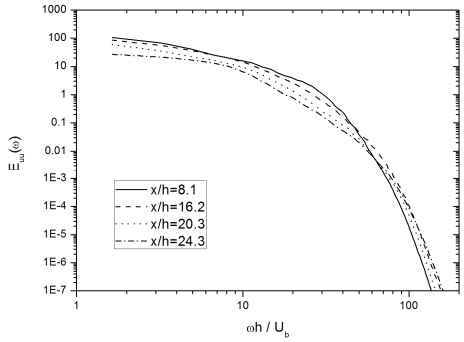

(b)

Fig. 6. Frequency spectra of streamwise velocity without forcing; (a) spectra in the vicinity of the wall; (b) spectra away from the wall.

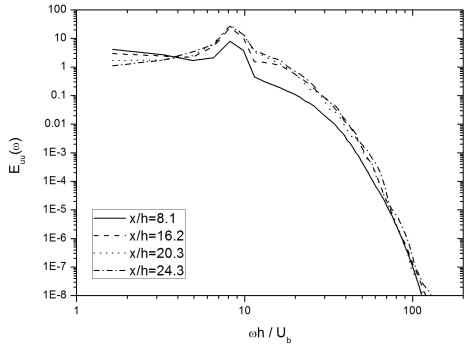

(a)

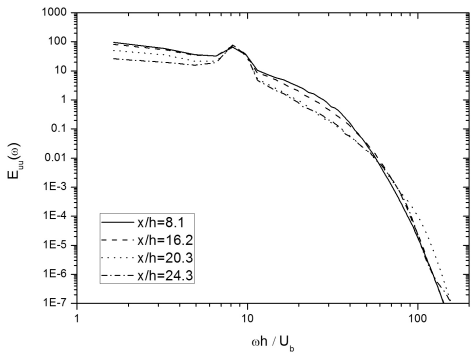

(b)

Fig. 7. Frequency spectra of streamwise velocity with forcing; (a) spectra in the vicinity of the wall; (b) spectra away from the wall.

of large-scale vortical structures is evident. More remarkable results can be found in Fig. 5, which traces the time history of pressure fluctuation with and without forcing. When the external disturbance was added, the pressure signal near the exit of the domain (*x/h*=24.3) showed highly organized frequency characteristics. The appearance of this time scale is a direct consequence of the imposition of disturbance with the same time scale in the velocity field. A more explicit revelation of the specified frequency in the pressure suggests that pressure is the variable most sensitive to the external excitation.

3.2 Frequency spectra

The flow behavior in the vicinity of the fuel surface is very important in the rocket motor because it is related to heat transfer mechanism, which directly affects the regression efficiency. In reality, the analysis of the flow near the surface is intimidating due to its complexity. The regression process causes the non-vertical momentum and the change in the local shape of the wall. Even with these complications, it is assumed that the basic flow physics is not likely to change significantly, and the variable geometry has a secondary effect. Thus, the response of external excitation in the frequency spectra was analyzed in the near-wall region.

Fig. 6 compares the frequency spectra of streamwise velocity at two different vertical locations with the case without forcing. In the vicinity of the wall, the spectra exhibit distinct peaks near the frequency of 8.5 after the injection started. The appearance of local maxima is clearly related to the action of the wall injection. As the flow moves downstream, amplification is further enhanced. Obviously, the corresponding frequency resulted from the shedding vortices. However, the effect of vortex shedding appears to diminish abruptly away from the wall, as shown in Fig. 6(b). This suggests that the effect of wall blowing is limited to the region very close to the wall. Somewhat different results were obtained when the external disturbance was imposed (Fig. 7). Distinctive peaks are prominent, and they are persistent even in the region away from the wall. The frequency imposed on the velocity field does not decay fast in the computational domain through the nonlinear interactions of the turbulence scales involved.

The turbulent temperature field treated as a passive scalar shows different behaviors (Figs. 8, 9). The effect of external disturbance is not manifested in both cases with and without disturbance. As shown in Fig. 3(c), the effect of external excitation is minimized in the temperature field, and this insensitivity is evident.

Fig. 10 shows the correlation between streamwise velocity and temperature. Regardless of external disturbance, the correlation in the vicinity of the wall is significantly lower than that in the region where wall injection is not applied. This behavior is expected from the results in Figs. 8-9. When the disturbance is introduced, the correlation drops throughout the channel

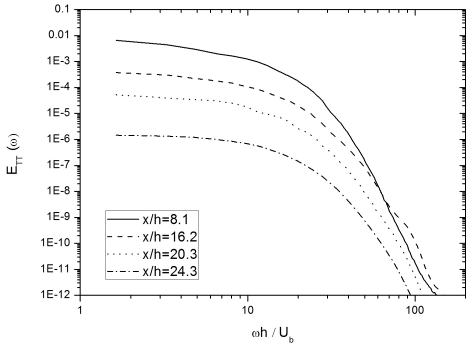

(a)

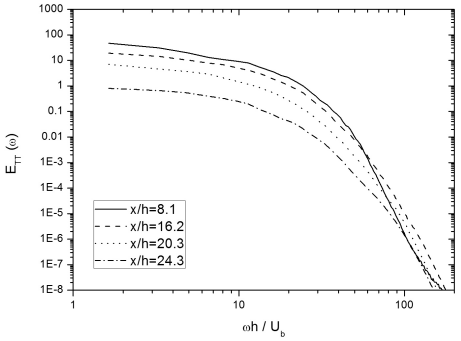

(b)

Fig. 8. Frequency spectra of temperature without forcing; (a) spectra in the vicinity of the wall; (b) spectra away from the wall.

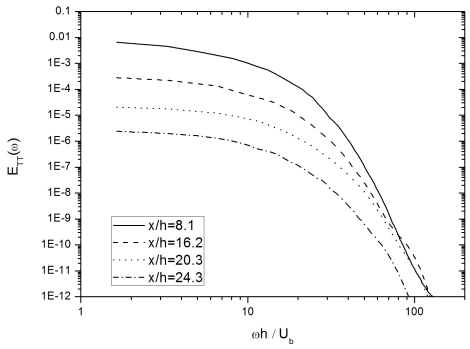

(a)

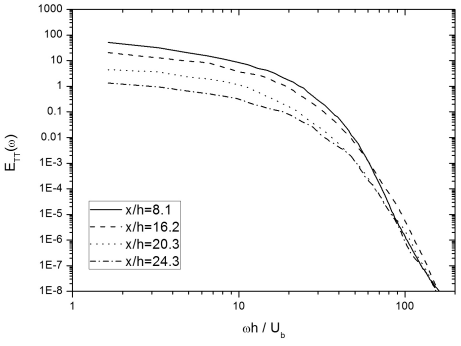

(b)

Fig. 9. Frequency spectra of temperature with forcing; (a) spectra in the vicinity of the wall; (b) spectra away from the wall.

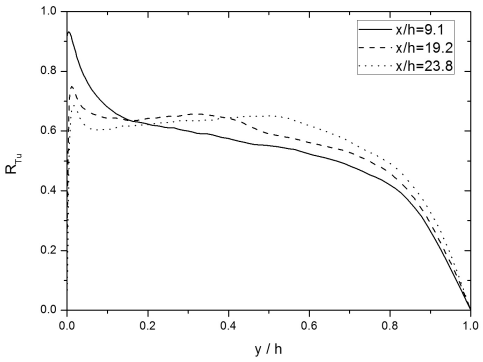

(a)

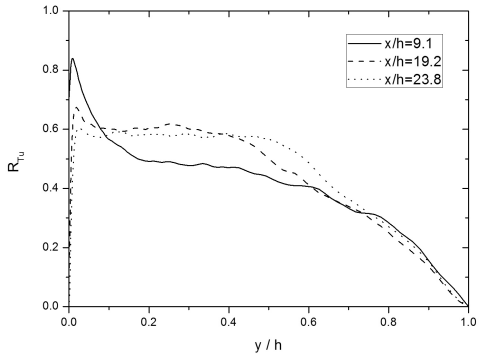

(b)

Fig. 10. Profiles of correlation coefficient between streamwise velocity and temperature; (a) case without forcing; (b) case with forcing.

height. As the dissimilarity is amplified through the introduction of external excitation, turbulence modeling for passive scalar would require a more sophisticated approach.

4. Conclusions

LES analysis was conducted in a transpired channel to investigate the effect of external disturbance. This flow configuration was relevant to that of a hybrid or a solid rocket motor. For the present study, concentrated momentum forcing was imposed to the flow to simulate the disturbance characterized by fixed frequency. Such form of excitation usually results from the geometric characteristics of a propulsion system, such as the shape of an injector. To simplify the computation, the chemical reaction was not considered, and thus the density variation was not considered.

More attention was given to the near-wall region where the behavior of heat transfer was of prime importance to the regression process. Results indicated that the concentrated momentum forcing at 8.5 agitated the pressure slightly, although the amplification was limited. That the current form of concentrated disturbance did not lead to resonance was thus concluded. The behavior of temperature was found to be very different from that of the velocity in the vicinity of the wall. Although the magnitude of the wall injection was restricted, it not only caused the dissimilarity between the velocity and temperature fields but also blowed the effect of external dis-

turbance in the temperature field away from the wall. This suggests that the classical approach, which assumes the constant turbulent Prandtl number, may not be useful in the present flow configuration, and a more sophisticated turbulence model is required for the temperature field. The higher sensitivity of the pressure to the external excitation compared with the velocity field still leaves room for the possibility of a sudden increase of flow instability. More effective ways of amplifying disturbance or prescribing a distributed forcing that simulates the white noise must be determined by future work.

Acknowledgment

This work of Y. Na was supported by the research project of the AETF program of Hanhwa, Inc. (2009).

Nomenclature

h : Half channel height
L_x, L_z : Domain size in the streamwise and spanwise directions
p : Pressure
p' : Pressure fluctuation
q_j : Residual heat flux vector
R_{Tu} : Correlation for streamwise velocity and temperature
t : Time
T : Temperature
T_{rms} : Root mean square of temperature fluctuation
T_w : Wall Temperature
u, v, w : Velocity component in x, y, z directions
u_{rms} : Root mean square of streamwise velocity
x, y, z : Cartesian coordinate in streamwise, wall-normal and spanwise directions
α : Thermal diffusivity
ν : Kinematic viscosity
τ_{ij} : Residual stress tensor

References

[1] K. Yamada, M. Goto and N. Ishikawa, Simulative study on the erosive burning of solod rocket motors, *AIAA Journal*, 14 (9) (1976) 1170-1176.
[2] J.-C. Traineau, P. Hervat and P. Kuentzmann, Cold flow simulation of a two dimensional nozzleless sold rocket motor, *AIAA Paper, 86-1447* (1986).
[3] R. Dunlap, A. M. Blackner, R. C. Waugh, Brown, R. S. and P. G. Willoughby, Internal flow field studies in a simulated cylindrical port rocket chamber, *Journal of Propulsion and Power*, 6 (6) (1990) 690-704.
[4] F. E. C. Culick, Rotational axisymmetric mean flow and damping of acoustic waves in solid propellant rocket motors, *AIAA Journal*, 4 (8) (1966) 1462-1464.
[5] B. Evans, N. A. Favorito and K. K. Kuo, Oxidizer-type and aluminum particle addition effects on solid fuel burning behavior, *AIAA Paper, 2006-4676* (2006).
[6] R. A. Beddini, Injection-induced flows in porous-walled ducts, *AIAA Journal*, 24 (11) (1986) 1766-1772.
[7] J. S. Sabnis, H. J. Gibeling and H. McDonald, Navier-Stokes analysis of solid propellant rocket motor internal flows, *Journal of Propulsion and Power*, 5 (6) (1989) 657-664.
[8] T.-M. Liou and W.-Y. Lien, Numerical simulation of injection driven flows in a two dimensional nozzles solid rocket motor, *Journal of Propulsion and Power*, 11 (4) (1995) 600-606.
[9] S. Apte and V. Yang, Unsteady flow evolution in porous chamber with surface mass injection, Part 1: Free Oscillation, *AIAA Journal*, 39 (8) (2001) 1577-1585.
[10] S. Apte and V. Yang, A large-eddy simulation study of transition and flow instability in a porous walled chamber with mass injection, *Journal of Fluid Mechanics*, 477 (2003) 215-225.
[11] Y. Na and C. Lee, Intrinsic flow oscillation in channel flow with wall blowing, *AIAA Paper, 2008-5019* (2008).
[12] C. Lee and Y. Na, Large eddy simulation of flow development in chamber with surface mass injection, *Journal of Propulsion and Power*, 25 (1) (2009) 51-59.
[13] Y. Na, Analysis on turbulent scalar field in a channel with wall injection using LES technique, *Journal of the Korean Society of Propulsion Engineers*, 13 (2) (2009) 54-63.
[14] Y. Na, Direct numerical simulation of turbulent scalar field in a channel with wall injection, *Numerical Heat Transfer, Part A*, 47 (2005) 165-181.
[15] T. Lund, X. Wu and K. D. Squires, Generation of turbulent inflow data for spatially developing boundary layer simulation, Journal of Computational Physics, 140 (2) (1998) 233-258.
[16] J. Adrian, Formation of coherent packets in wall turbulence, *Self sustaining Mechanism of Wall Turbulence,* edited by R. L. Panton, Computational Mechanics Publications, Boston, Ma, (1997) 109-134.

Dongshin Shin received his B.S. and M.S. in Mechanical Engineering from Seoul National University in Korea, in 1983 and 1985, respectively. He then received his Ph.D. degree from Stanford University in the US, in 1992. Dr. Shin is currently a Professor at the School of Mechanical System Design Engineering at Hongik University in Seoul, Korea. He is the Associate Editor of the Journal of Mechanical Science and Technology. His research interests include turbulence, instability, combustion, and computational fluid dynamics.

Yang Na received his B.S. and M. S. degrees in mechanical engineering from Seoul National University, Korea and his Ph. D. degree from Stanford University in the US. His research interests are in the areas of turbulence, computational fluid dynamics, and convective heat transfer.